Supplementary Material for: Generative Adversarial Networks (GANs): Challenges, Solutions, and Future Directions

DIVYA SAXENA, University Research Facility in Big Data Analytics (UBDA), The Hong Kong Polytechnic University, Hong Kong
JIANNONG CAO, Department of Computing and UBDA, The Hong Kong Polytechnic University, Hong Kong

1 RE-ENGINEERED NETWORK ARCHITECTURE

1.1 Conditional Generation

Further discussion. Table 1 shows objective function of conditional GANs. Conditional GANs mainly handling the mode collapse challenge by conditioning the model on additional information. In addition, generally cGANs are based on the supervised learning [1–4]. We also find that conditional GANs has been used for the several applications, such as **image generation (IG)**, image tag recommendation, compression, and so on, which shows that vast number of applications require that data is conditionally generated from certain data mode(s).

We have already discussed in Section 3 that selection of right evaluation metric is critical factor for making the right conclusion just like selection of a training method is crucial for accomplishing high performance in an application. References [1, 5] have used Log-likelihood (or equivalently KL divergence), a de facto standard for training and evaluating generative models. It is considered that model with maximum likelihood generates better samples. Reference [6] has explored most widely adopted **Inception Score (IS)** [7] and **Multi-Scale Structural Similarity Index (MS-SSIM)** [8] metric for GANs evaluation. IS mainly captures the two main properties of generated samples: highly classifiable and diverse w.r.t. class labels. This score shows correlation with the quality and diversity of generated samples. MS-SSIM is one of the image quality measures that only consider visual fidelity and do not consider diversity of samples. Precision, Recall, and F1-score are applied for computing degree of overfitting in GANs. Reference [6] has used SSIM as evaluation measure, which only considers visual fidelity instead of diversity of generated samples. While Reference [9] used human evaluation as evaluation measure, which cannot completely measure the capacity of models.

1.2 Generative-discriminative Network Pair

1.2.1 Training of Single Generator

Further discussion. Normalization of D is valuable from both the optimization (more efficient gradient flow, a more stable optimization) and representation perspectives. In GANs literature, several techniques have been introduced from the optimization perspective, namely, **batch normalization (BN)** [10] and **layer normalization (LN)** [11]. DCGAN popularized the use of Batch normalization in the GANs framework, while Layer normalization is used in GANs framework by Reference [12].

0360-0300/2021/05-ART63 $15.00
https://doi.org/10.1145/3446374

Table 1. Objective Function of Conditional Generation

Model	Loss Type	Loss Function	Description
cGANs [1]	Conditional Loss	$\mathbb{E}_{x\sim p_{data}}[log(D(x, c))] + \mathbb{E}_{z\sim p_z}[\log(1 - D(G(z, c), c))]$	c is a condition.
IRGAN [5]	Conditional loss + Regularization	$\mathbb{E}_{x\sim p_{data}(x)}[log(D(x, c))] + \mathbb{E}_{z\sim p_z, c\sim p_{data}(c)}[\log(1 - D(G(z, c), c))] + R(G)$ $R(G) = -\lambda\mathbb{E}_{c\sim p_{data(c)}, x\sim G(z,c)}[\log Q(c\|x)]$	$R(G)$ is defined by the lower bound [41] of the mutual information $I(c;\ G(z,\ c))$ where c is sampled from the data distribution rather than a pre-defined distribution. Approximator $Q(c\|x)$ measures $p(c\|x)$ from x.
IcGAN [2]	Squared reconstruction loss	$L_{Ez} = \mathbb{E}_{z\sim p_z, y'\sim p_y}\|\|z - E_z(G(z,\ y'))\|\|_2^2$ $L_{Ey} = \mathbb{E}_{x,y\sim p_{data}}\|\|y - E_y(x)\|\|_2^2$	E is composed of two independent sub-encoders: E_z for encoding an image to z, and E_y for encoding an image to y. P_y is density model to sample generated labels y' for generated data x'.
BiCoGAN [3]	Extrinsic factor loss (EFL)	$\mathbb{E}_{x\sim p_{data(x)}}[\log(D(E(x), x))] + \gamma\mathbb{E}_{(x,c)\sim p_{data(x,\ c)}}[EFL(c, E(x))] + \mathbb{E}_{z\sim P_{\tilde{z}}(\tilde{z})}[\log(1 - D((\tilde{z}), G(\tilde{z})))]$	$\tilde{z}$=[z c] EFL is an explicit mechanism used to guide BiCoGANs for encoding extrinsic factors efficiently.
MatAN [4]	MatAN loss	$\mathbb{E}_{y_1, y_2\sim p_{data(x,y,t)}} \log D(T_1(\hat{y}), T_2(\hat{y}), \theta_M, b) + \mathbb{E}_{y_1, x\sim p_{data(x,y,t)}} log(1 - D(T_1(\hat{y}), T_g(G(x, \theta_G)), \theta_M, b))$	T_1, T_2, T_g might be the identity transformation, depending on the $T_i()$ configuration, θ_M id for Siamese network and b is a trained bias.
AC-GAN [6]	Conditional loss	$L_S = \mathbb{E}_{x\sim p_{data}}[\log D(x)]\ + \mathbb{E}_{z\sim p_z}[\log\ (1 -\ D(G(z)))]$ $L_C = \mathbb{E}_{x\sim p_{data}}[\log D(x, c)] + \mathbb{E}_{z\sim p_z}[\log(1 - D(G(z, c), c))]$	Log-likelihood of the correct source, L_S, and the log-likelihood of the correct class, L_C. D is trained to maximize $L_S + L_C$ while G is trained to maximize $L_C - L_S$.
TripleGAN [68]	Standard supervised loss (i.e., cross-entropy loss)	$E_{(x,y)\sim p_{data}(x,y)}[logD(x, y)] + \alpha E_{(x,y)\sim p_c(x,y)}[log(1 - D(x, y))] + (1 - \alpha)E_{(x,y)\sim p_z(x,y)}[\log(1 - D(G(y, z), y))] + R_L$ $R_L = E_{(x,y)\sim p_{data}(x,y)}[-\log p_c(y\|x)]$	$\alpha \in (0, 1)$ is a constant that controls the relative importance of generation and classification.
KDGAN [69]	Distillation loss	$\mathbb{E}_{y\sim p_{data}}[\log D(x,\ y)] + \alpha\mathbb{E}_{y\sim p_c}[log(1 - D(x, y)) + (1 - \alpha)\mathbb{E}_{y\sim p_t}[log(1 - D(x, y)) + \beta L_{DS}^c(C(y\|x), T(y\|x)) +\ \gamma L_{DS}^t(T(y\|x), C(y\|x))$	L_{DS}^t and L_{DS}^c are distillation loss. $\alpha\ \in (0,\ 1),\ \beta \in (0, +\infty)$, $\gamma \in (0, +\infty)$.
ControlGAN [9]	Classification loss	$\theta_D = argmin\{\alpha L_D(t_D, D(x; \theta_D)) + (1 - \alpha)L_D((1 - t_D), D(G(z, l; \theta_G); \theta_D))\}$ $\theta_G = argmin\{\gamma_t.L_C(l, G(z, l; \theta_G)) + L_D((t_D, D(G(z, l; \theta_G), \theta_D)))\}$ $\theta_C = argmin\{L_C(l, x; \theta_C)\}$	l is the binary representation of labels of sample x and input data for the G, t_D is the label for D and set to 1, and α denotes a parameter for the D. γ_t is a learning parameter.

Table 2. Objective Function of Single Generator-based GANs

Model	Loss Type	Loss Function	Description
LAPGAN [65]	–	$\mathbb{E}_{x,\, l\sim p_{data}}[\log D(x, l)] + \mathbb{E}_{z\sim p_z, l\sim p_l}[\log (1 - D(G(z, l)))]$	Used cGANs approach at each level l of the pyramid. p_l is the prior distribution over classes.
DCGANs [13]	Cross Entropy Loss	$\mathbb{E}_{x\sim p_{data}}[\log D(x)] + \mathbb{E}_{z\sim p_z}[\log (1 - D(G(z)))]$	–
SGAN [66]	Conditional Loss (G) + Entropy Loss (G)	$\mathbb{E}_{h_i\sim p_{data},\, E}[-\log D_i(h_i)] +$ $\mathbb{E}_{z_i\sim p_{z_i},\, h_{i+1}\sim p_{data},\, E}[-\log(1 - D_i(G_i(h_{i+1},\, z_i)))] +$ $\mathbb{E}_{z_i\sim p_{z_i},\, h_{i+1}\sim p_{data},\, E}[f(E_i(G_i(h_{i+1},\, z_i)),\, h_{i+1})] +$ $\mathbb{E}_{z_i\sim p_{z_i}}[\mathbb{E}_{\hat{h}_i\sim G_i(\hat{h}_i\|z_i)}[-\log Q_i(z_i\|\hat{h}_i)]$	h is hierarchical level. f is a Euclidean distance measure for intermediate representations and cross-entropy for labels. SGAN used an auxiliary distribution $Q_i(z_i\|\hat{h}_i)$ to approximate the true posterior $P_i(z_i\|\hat{h}_i)$.
ProgressGAN [14]	WGAN-GP loss and LSGAN loss	–	–
PacGAN [15]	Total Variation (TV) Distance	$L_D = \log(1 + \exp(-\mathrm{D}(x))) + \log(1 + \exp(\mathrm{D}(x')))$ $L_G = \log(1 + \exp(\mathrm{D}(x))) + \log(1 + \exp(-\mathrm{D}(x')))$	x' is generated data. Packed samples as a single sample that is drawn from the product distribution.
BayesianGAN [17]	–	$\theta_D^{j,m} = \theta_D^{j,m} + \upsilon_D$ $\theta_G^{j,m} = \theta_G^{j,m} + \upsilon_G$ $\upsilon_D = (1-\alpha)\upsilon + \eta\left(\sum_{i=1}^{J_D}\sum_{k=1}^{J_G}\frac{\partial\, log\, p(\theta_D\|z^i, x, \theta_G^{k,m})}{\partial\theta_D}\right) + n$ $\upsilon_G = (1-\alpha)\upsilon + \eta\left(\sum_{i=1}^{J_G}\sum_{k=1}^{J_D}\frac{\partial\, log\, p(\theta_G\|z^i, x, \theta_D^{k,m})}{\partial\theta_G}\right) + n$ $\mathrm{n} \sim \mathcal{N}(0,\ 2\alpha\eta I)$	α is the friction term for Stochastic Gradient Hamiltonian Monte Carlo (SGHMC), η is the learning rate. $\mathrm{J_G}$ and $\mathrm{J_D}$ are simple MC samples for the G and D, respectively, and m is SGHMC samples for each simple MC sample.
CapsNets [18]	Margin Loss	$L_D = \mathbb{E}_{x\sim p_{data}}[-L_M(D(x),\ T = 1)] + \mathbb{E}_{z\sim p_z}[-L_M(D(G(z)),\ T = 0)]$ $L_M = \sum_{k=1}^{K} T_k \max(0,\ m^+ - V_k)^2 + \lambda(1 - T_k)\max(0,\ V_k - m^-)^2$ $L_G = \mathbb{E}_{z\sim p_z}[-L_M(D(G(z)), T = 1)]$	T_k represents target labels. m^+, m^-, and λ are down-weighting factor to prevent initial learning from shrinking lengths of the capsule outputs in the final layer. V_k is vector outputs of the final layer.
SAGAN [19]	Hinge version of the adversarial loss	$L_D = -\mathbb{E}_{(x,y)\sim p_{data}}[min(0,\ -1 + D(x, y))] - \mathbb{E}_{z\sim p_z, y\sim p_{data}}[min(0, -1 - D(G(z), y))]$ $L_G = \mathbb{E}_{z\sim p_z, y\sim p_{data}}[D(G(z), y)]$	–

Table 2 shows objective function of single generator-based GANs. Current approaches have mainly targeted the development of solutions for the mode collapse challenge using different architectural layers and networks. In addition, the scale at which each of the proposed architecture improves the stability of the GANs is quite different. We find that most of the works [13–19] of the developing new architectural GANs has mainly focused on the **image generation (IG)** and classification applications. DCGAN has demonstrated better training stability and is one of the most popular GANs variants in the literature. DCGANs has used the classification error rate for the evaluation where this metric deeply depends on the selection of a classifier. DCGANs has made use of nearest neighbor classifiers where Euclidean distance is not a suitable dissimilarity measure for images. Reference [16] proposed a new evaluation metric, **Generative Adversarial Metric (GAM)**, to evaluate the model quantitatively.

Table 3. Objective Function of Multiple Generators-based GANs

Model	Loss Type	Loss Function	Description
cGAN [70]	Cross Entropy loss	$Q(x_k) = \begin{cases} 1 & D(x) > t_r \\ 0 & else \end{cases}$	Used gate-function Q for redirecting data to the next GANs, $Q(x_k) = 1$ means transfer the data to the next GANs, otherwise not.
AdaGAN [71]	Binary Cross Entropy loss	$\mathbb{E}_{x \sim p_{data}}[logD(x)] + \mathbb{E}_{z_1 \sim p_{z_1(z_1)}}[\log(1 - D(G_1(z_1)))] + \mathbb{E}_{z_2 \sim p_{z_2(z_2)}}[\log(1 - D(G_2(z_2)))] \mathbb{E}_{x \sim p_z(z), enc[msg(G_2(z_2, m_1)), z_2, m_1]]} [\log(1 - D(G_1(x)))] - f(D(G_1(x))) - D(G_2(x))$	For G_1, and similar version for G_2.
MAD-GAN [72]	Multi-label cross entropy loss	$\mathbb{E}_{x \sim p_{data}}[\phi(D_v(x))] + \mathbb{E}_{x \sim p_z}[\phi(1 - D_v(x))]$	ϕ is a measuring function $\phi : [0, 1] \rightarrow \mathbb{R}$, u $\in U$ and $v \in V$.
MGAN [73]	Standard Softmax loss	$\mathbb{E}_{x \sim p_{data}}[\log D_{k+1}(x; \theta_d)] + \mathbb{E}_{z \sim p_z}[\log(1 - D_{k+1}(G_i(z; \theta_g^i); \theta_d)]$	Dj(x; θ_d) is jth index of D(x; θ_d) for which $\delta(j) = 1$. A standard softmax loss is used for a multi-classification to maximize the entropy for the classifier.
MPM GAN [74]	–	$\mathbb{E}_{x \sim p_{data}}[\log\ D(x)] + \mathbb{E}_{x \sim p_z}[\log(1 - D(x))] - \beta\{\sum_{k=1}^{K} \pi_k \mathbb{E}_{x \sim p_{G_k}}[\log C_k(x)\}$	Each G_k maps z to $x = G_k(z)$, thus inducing a single distribution p_{G_k}. $C_k(x)$ is the probability that x is generated by G_k and $\beta > 0$ is the diverse hyperparameter.
Fictitious GAN [75]	–	$\mathbb{E}_{x \sim p_{data}}[f_0(D(x))] + \mathbb{E}_{x \sim p_z}[f_1(D(G(x)))]$	$f_0(\cdot)$ and $f_1(\cdot)$ are some quasi-concave functions depending on the GANs variants.
MIX+GAN [76]	–	$\mathbb{E}_{x \sim p_{data}}\ [\log(D_i(x))] + \mathbb{E}_{z \sim p_z}[\log\ (1 -\ D_i(G(z)))]$	–

1.2.2 *Training of Multiple Generators*

Further discussion. Table 3 shows objective function of multiple generators-based GANs. Most of the current approaches of the multiple Gs have proposed solutions for mitigating the mode collapse problem. Majority of the work has evaluated the proposed multi-agent architecture for the image generation application. Proposed solutions have shown promising results but not state-of-the-art results. Most of the works have used the well-known evaluation metric, **Inception Score (IS)**.

1.2.3 *Training of Multiple Discriminators*

Further discussion. Table 4 shows objective function of multiple discriminators-based GANs. Most of the works have used the well-known evaluation metric, **Inception Score (IS)**. Reference [20] has proposed a new metric, called **Generative multi-adversarial metric (GMAM)**. GMAM is an extension of GAM [16] to train multiple Ds. Reference [21] used mode score, which is quite similar to IS metric. Mode score also consider prior distribution of the labels over training data. Reference [22] have used **Frećhet Inception Distance (FID)**, a metric to calculate the Wasserstein-2 distance between the generated and real distributions to find the generated samples quality.

1.3 Joint Architecture

1.3.1 *Data space Autoencoders*

Further discussion. Recently, three classes of algorithms—**(Variational) Auto Encoders (AEs and VAEs)**, autoregressive approaches, and deep GANs—have shown potential for learning deep

Table 4. Objective Function of Multiple Discriminators-based GANs

Model	Loss Type	Loss Function	Description
D2GAN [21]	Symmetric KL divergence and Wasserstein distance	$\alpha\mathbb{E}_{x\sim p_{data}}[\log D_1(x)] + \mathbb{E}_{z\sim p_z}[-D_1(G(z))] + \mathbb{E}_{x\sim p_{data}}[-D_2(x)] + \beta\mathbb{E}_{z\sim p_z}[log\ D_2(G(z))]$	$0 < \alpha, \beta \leq 1$.
GMAN [20]	Cross Entropy loss	$\mathbb{E}_{x\sim p_{data}}[\log D(x)] + \mathbb{E}_{z\sim p_z}[\log (1 - D(G(z)))]$	–
StabGAN [77]	–	$\sum_{i=k}^{K} \mathbb{E}_{x\sim p_{data}}[\log D_k(W_k^T x)] + \mathbb{E}_{Z\sim p_Z}[\log(1 - D_k(W_k^T G(z)))]$	$W_k, k \in \{1, \ldots., K\}$ is a randomly chosen matrix in $\mathbb{R}^{d*m}$ with $m < d$.
Dropout GAN [78]	–	$\sum_{i=k}^{K} \delta_k(\mathbb{E}_{x\sim p_{data}(x)}[logD_k(x)] + \mathbb{E}_{z\sim p_z(z)}log(1 - D_K(G(z))))$	δ_k is a Bernoulli variable ($\delta_k \sim$ Bern (1 − d)) and $\{D_k\}$ is the set of K total Ds.
SGAN [22]	Wasserstein loss	$L_G = \mathbb{E}_{z\sim p_z}[\log(D(G(z)))]$	Objective function for L_D is not defined.

directed generative models. Autoregressive approaches model the relationship between input variables directly and produce outstanding samples. However, autoregressive models [23–25] suffer from the slow sampling speed. GANs can learn a unidirectional mapping to generate samples from the data distribution without foregoing sampling speed and also makes use of a latent representation in the generation process while VAEs includes both generation and inference as it learns a bidirectional mapping between a complex data distribution and simple prior distribution. The combination of VAE and GANs come with several benefits, such as solutions can be used to reconstruct data, inference network supports representation learning, and so on. Models based on the combination of VAE and GANs can be used for unsupervised, supervised, and reinforcement learning.

Table 5 shows objective function of data space autoencoders. References [26, 31, 32, 75] autoencode data points. Due to this, the selection of a good loss function over natural images is a challenging task. In data-space autoencoders, only Reference [30] has tried to handle both gradient vanishing and mode collapse problems in the GANs training, while remaining works have handled only the mode collapse problem. The combination of VAE and GANs provides promising results in terms of handling mode collapse, but still it has not been explored much.

These research works mainly focus on the image generation. Reference [31] has used a metric **negative log-likelihood (NLL)**, estimated via the variational lower bound for natural images. Reference [31] has evaluated proposed solution on both reconstruction and generation. Reference [32] has used independent Wasserstein critic, which calculates both mode collapse and overfitting in which if G remembers the training data, the critic trained on the validation set can differentiate between generated samples and data, and if mode collapse strikes, critic can easily separate generated samples from the data.

1.3.2 *Latent space Autoencoders*

Further discussion. Table 6 shows objective function of latent space autoencoders. In basic GANs, efficient inference mechanism does not exist. Reference [33] proposed to learn generation and inference network jointly in an adversarial way. Moreover, Reference [34] training has shown that *inverse* objective delivers more strong gradient signal to E and G and makes the training stable.

Most of the works in latent space autoencoder focus on the diversity of the generated images. Reference [38] has used a new **inference via optimization metric (IvOM)** metric in which

Table 5. Objective Function of Data Space Autoencoders

Model	Loss Type	Loss Function	Description
VAE-GAN [27]	Prior regularization term + reconstruction error (D)	$L_{GAN} = \log(D(x)) + \log(1 - D(Dec(z))) + \log(1 - D(Dec(E(x))))$ $L_{prior} = D_{KL}(q(z\|x)\|\|p(z))$ $L^{D}_{llike} = -\mathbb{E}_{q(z\|x)}[\log p(D_l(x)\|z)]$	$D_l(x)$ denote the hidden representation of the lth layer of the D.
AAE [28]	Reconstruction error + adv. training	–	Adversarial training procedure in which q(z) is matched to the whole distribution of p(z).
AVB [29]	–	$L_D = \max_D \mathbb{E}_{p_d(x)} \mathbb{E}_{q_\phi(z\|x)} \log \sigma(D(x, z)) + \mathbb{E}_{p_d(x)} \mathbb{E}_{p(z)} log(1 - \sigma(D(x, z)))$	Objective for the $D(x, z)$ for a given $q_\phi(z\|x)$.
ASVAE [31]	–	$\min_{\theta,\ \phi} \max_{\psi_1,\ \psi_2} -3\mathcal{L}_{VAE_{xz}}(\theta,\ \phi,\ \psi_1,\ \psi_2)$ $\mathcal{L}_{VAE_{xz}}(\theta,\ \phi,\ \psi_1,\ \psi_2) = \mathbb{E}_{x\sim q(x),\ \epsilon\sim N(0,I)}[f_{\psi_1}(x, z_\phi(x, \epsilon)) - log_{p_\theta}(x\|z_\phi(x, \epsilon))] + \mathbb{E}_{z\sim p(z),\ \epsilon\sim N(0,I)}[f_{\psi_2}(x_\theta(z,\ \xi), z) - log_{q_\phi}(z\|x_\theta(z,\ \xi))]$	The expectations are approximated via samples drawn from $q(x)$ and $p(z)$, as well as samples of ϵ and ξ.
MDGAN [26]	Regularization with loss	$L_G = -\mathbb{E}_z[\log D(G(z))] + \mathbb{E}_{x\sim p_d}[\lambda_1 d(x, G\ o\ E(x)) + \lambda_2 \log D(G\ o\ E(x))$ $L_E = \mathbb{E}_{x\sim p_d}[\lambda_1 d(x, G\ o\ E(x)) + \lambda_2 \log D(G\ o\ E(x))$	G ° E is an autoencoder.
Dist-GAN [30]	Latent-data distance constraint + discriminator-score distance constraint	$L_G = \lvert\mathbb{E}_x \sigma(D(x)) - \mathbb{E}_z \sigma(D(G(z)))\rvert$ $L_D = -(\mathbb{E}_x log\sigma(D(x)) - \mathbb{E}_z log(1 - \sigma(D(G(z)))) + \mathbb{E}_x log\sigma(D(G(E(x)))) - L_p)$ $L_p = \lambda_p \mathbb{E}_{\hat{x}}(\nabla_{\hat{x}} D(\hat{x})_2^2 - 1)^2$	Applied the gradient penalty L_p for the D_γ objective, where λ_p is penalty coefficient, and $\hat{x} = \epsilon x + (1 - \epsilon)G(z)$, ϵ is a uniform random number $\epsilon \in U[0, 1]$.
α-GAN [32]	Hybrid loss	$\mathcal{L}(\theta, \eta) = \mathbb{E}_{q_\eta(z\|x)}\Big[- \lambda x - \mathcal{G}_\theta(z)_1 + \log \frac{\mathcal{D}_\phi(\mathcal{G}_\theta(z))}{1-\mathcal{D}_\phi(\mathcal{G}_\theta(z))} + log\ \frac{C_\omega(z)}{1-C_\omega(z)}\Big]$	$\mathcal{L}(\theta, \eta)$ is the hybrid loss function where $\mathcal{D}_\phi(x)$ is a classifier and C_ω is a latent classifier.

samples from the test data are compared to the nearest generated sample. If G undergoes mode collapse, then for some images distance is large.

1.4 Improved Discriminator

Further discussion. Table 7 shows objective function of improved discriminator-based GANs. Energy-based GANs has explored the GANs framework from the energy-based perspective. Energy-based GANs are supposed to increase the quality and variety of generated images. Moreover, these GANs have shown good convergence pattern and scalability for generating higher-resolution images. However, in these solutions visual modes are not boosted. Energy-based GANs works for both image quality and diversity of the images. Apart from it, all current approaches of the energy-based GANs have mainly targeted the instability challenge. Energy-based GANs model has focused on the image generation application. Also, most of the works have used **Inception Score (IS)** as evaluation metric.

1.5 Latent Space Engineering

Further discussion. Table 8 shows objective function of latent space engineering-based GANs, i.e., noise-engineered GANs. They have primarily handled the issue of mode collapse while

Table 6. Objective Function of Latent Space Autoencoders

Model	Loss Type	Loss Function	Description
ALI [33]	–	$\mathbb{E}_{q(x)}[\log(D(x, G_z(x)))] + \mathbb{E}_{p(x)}[\log(1 - D(G_x(z), z))]$	ALI's objective is to match the two joint distributions.
BiGAN [34]	–	$\mathbb{E}_{q(x)}[\log(D(x, E(x)))] + \mathbb{E}_{p(x)}[\log(1 - D(G(z), z))]$	Optimize this minimax objective using the same alternating gradient based optimization as Reference [35].
HALI [36]	–	$L_D = \frac{1}{M}\sum_{i=1}^{M}\log({p_q}^{(i)}) - \frac{1}{M}\sum_{i=1}^{M}\log(1 - {p_p}^{(i)})$ $L_G = \frac{1}{M}\sum_{i=1}^{M}\log(1 - {p_q}^{(i)}) - \frac{1}{M}\sum_{i=1}^{M}\log({p_p}^{(i)})$	p_q is used to get D's predictions on E's distribution and p_p is used to get D's predictions on D's distribution.
AGE [37]	–	$\Delta(E(G(z)))\|\|E(x)$	Generate a distribution G(z) in data space that is close to the real data distribution x.
VEEGAN [38]	logistic regression loss	$-\mathbb{E}_{\gamma}[\log(D_\omega(z, x))] - \mathbb{E}_{\theta}[\log(1 - D_\omega(z, x))]$	Eγ is expectation w.r.t. the joint distribution qγ(x|z)p(x) and Eθ w.r.t. pθ(z|x)p(x).
MGGAN [39]	–	$\mathbb{E}_{x\sim p_{data}}[\log D_x(x) + \log D_m(E(x))] + \mathbb{E}_{z\sim p_z}[\log(1 - D_x(G(z))) + \log(1 - D_m(E(G(z))))]$	Dm is a discriminator for the guidance network and m means manifold space. Two Ds, Dx and Dm, do not explicitly affect each other, but both of them influence G.

Table 7. Objective Function of Improved Discriminator-based GANs

Model	Loss Type	Loss Function	Description
EBGAN [79]	Hinge loss	$L_D = D(x) + [m - D(G(z))]^+$ $L_G = D(G(z))$	here $[\cdot]+ = \max(0, \cdot)$.
BEGAN [80]	–	$L_D = L(x) - k_t\alpha(G(z_D))$ $L_G = L(G(z_G))$	$k_t \in [0, 1]$ to control $L(G(z_D))$ during gradient descent.
MAGAN [81]	Adaptive hinge loss	$L_D = D(x) + \max(0,\ m - D(G(z)))$ $L_G = D(G(z))$	D(x) is a deep auto-encoder function.
Max-Boost-GAN [82]	Margin loss	$L_D = D(G(x)) + [\max(D(G(z_1)), D(G(z_2))) - m]^+$ $L_G = \max(D(G(z_1)), D(G(z_2)))$	m is a positive margin.

Reference [40] has focused for the convergence of the training to make the model more robust. Reference [41] proposed a solution for minimizing the mutual information between a subset c of the latent code and x by using an auxiliary distribution Q($c|x$). However, InfoGAN does not support full inference on z, i.e., only the value for c is inferred.

Noise-engineered GANs models have tackled a variety of applications. Furthermore, Reference [42] has introduced **modified Inception Score (m-IS)** by adding cross-entropy style score in the original IS metric. Reference [40] introduced **Frechet Classification Distance (FCD)** to compute quality of generated images. Authors have also provided an analysis that a low value of FCD and high values of the clustering metrics (clustering accuracy (ACC), **normalized mutual information (NMI)**, and **adjusted rand index (ARI)**) show that generated data is near to the real data and generated modes are matched with real data modes.

Table 8. Objective Function of Latent Space Engineering based GANs

Model	Loss Type	Loss Function	Description
DeliGAN [42]	L2 regularization	$L_{GAN} = \mathbb{E}_{x\sim p_{data}}[\log D(x)] + \mathbb{E}_{z\sim p_z}[log\ (1 - D(G(z)))] \mathbb{E}_{z\sim p_z}[log\ (1 - D(G(z)))] + \lambda \sum_{i=1}^{N} \frac{(1-\sigma_i)}{N}$	N is the number of Gaussian Component and $\sigma_i = 0.2$.
NEMGAN [40]	Categorical cross-entropy loss	$L(G,\ h_1,\ h_2,\ D) = \mathbb{E}_{x\sim p_{data}}[log\ D(x)] + \mathbb{E}_{z\sim p_z}[log(D\ o\ G(z)) + \|\|z - h_1\ o\ G(z)\|\|p] + D_{KL}(P_{\hat{Y}}\|\|P_Y)$ $L_{GAN} = L(G,\ h_1,\ h_2,\ D) + \min_h L_{CC} + \min_\alpha D_{KL}(P_{\hat{Y}}\|\|\hat{P}_{\hat{Y}})$	The inversion network h2(h1(g(z))) inverts the generation process to ensure the matching of modal properties of generating and latent distributions. $\mathbb{E}_z[h(x)] = P_{\hat{Y}}$.
DE-GAN [84]	Hidden-space loss	$L_{GAN} = \mathbb{E}_{x\sim p_{data}}[\log D(x)] + \mathbb{E}_{z\sim p_z}[log\ (1 - D(G(z)))]$ Hidden space loss = $\frac{1}{N}\sum_{i=1}^{N} h^i(X_{real}) - h^i(X_{gen})$	$h(X_{real})$ represents the activation map of a high convolutional layer when a real image is sent to D, while $h(X_{gen})$ denotes a generated one.
InfoGAN [41]	Information-theoretic regularization	$\mathbb{E}_{x\sim p_{data}}[\log D(x)] + \mathbb{E}_{z\sim p_z}[\log\ (1 - D(G(z)))] - \lambda I(c; G(z, c))$	–

2 NEW LOSS FUNCTION

To highlight the contribution of solutions proposed under this section, we provide a summary including concerns raised in the article, approaches used to handle those concerns, and strengths and limitations of the proposed solution. We believe this summary will be useful for the future researchers to understand the progress of loss functions for GANs well. Tables 9 and 10 show the summary of proposed probability distance and divergence and regularization schemes for GANs, respectively.

3 SUMMARY

In Table 11, we summarize GANs design and optimization solutions proposed for handling two main GANs challenges: **mode collapse (MC)** and **non-convergence and instability (NC&I)**. The first and second column state the challenges addressed in the article. The rest columns show the proposed solutions in the article for handling the addressed GANs challenge(s) (as shown in Table 1 in main document).

4 APPLICATIONS OF GANS

Research on GANs is rapidly growing, and several GANs variants have been proposed focusing on various aspects of deep learning. These variants have demonstrated the potential of GANs and have shown promise for developing a broad number of interesting and useful applications in several research domains, such as image generation, domain transfer, data generation, ethics in AI, and so on. In this section, we shall point out main GANs applications within these major research domains.

4.1 Image Generation

Recently, GANs has gained more and more momentum for generating naturalistic images through adversarial training. Reference [85] studied the problem of image generation from different points of view. Authors claimed that visual appearance of objects is significantly influenced by their shape geometry, which has not been considered by any of the existing works for image generation. To

Table 9. Summary of Probability Distance and Divergence for GANs

Models	Concerns Raised	Approach	Strengths	Limitations
WGAN [43]	Vanishing Gradient. Requires D to learn 1-Lipschitz functions.	Minimizes a reasonable and efficient approximation of the EM distance or Wasserstein-1. Enforce the Lipschitz constrained by weight clipping.	A meaningful loss metric that correlates with the G's convergence and sample quality. An improved stability of the optimization process. It does not require a careful design of the network architecture either. The mode-dropping phenomenon that is typical in GANs is also drastically reduced.	Unstable when gradients of the loss function are large. Slow training. Tuning weight clipping and hyperparameters is a tedious task. It does not consider to increase the variety of mode of generated visual samples and the variety of semantics of visual samples.
LS-GAN [44]	G suffers from vanishing gradient, as D can be optimized very quickly. Assuming infinite capacity for convergence, which leads to mode collapse.	Uses a Lipschitz constraint but reason is independent of WGAN's Lipschitz condition. Uses a weight-decay regularization technique. Loss having a data-dependent margin with gradients everywhere. Convergence proof without the assumption of infinite capacity. Generalization bounds.	Due to Lipschitz regularity, LS-GAN can generalize well to produce new data from training examples.	It does not increase the variety of mode of generated visual samples and the variety of semantics of visual samples.
RWGAN [45]	Lack of robustness and efficiency during the learning process.	Proposed a new class of statistical divergence, RW divergence, a combination of Bregman divergence and Wasserstein divergence. Asymmetric clipping.	Due to Asymmetric clipping, avoids the low-quality samples and the failure of convergence. Wasserstein-L2 distance of order 2 improves the speed of convergence.	–
f-GAN [46]	Generalize GANs objective to variational divergence minimization	Minimizes the variational estimate of f-divergence. Simplify the saddle-point optimization [] and provide a theoretical justification.	Learning objective is effective and computationally inexpensive than GANs.	Use of Generative neural samplers is limited, because after training they are unable to provide inferences.
b-GAN [47]	GANs are sensitive to datasets, the form of the network, and hyperparameters. In GANs, the value function derived from the two-player minimax game does not match the objective function.	Objective function derived from the original motivation is not changed for learning the generative model. Learn a deep generative model from a density ratio estimation perspective. Pearson divergence.	Improve the stability of GANs learning.	–

(Continued)

Table 9. Continued

Models	Concerns Raised	Approach	Strengths	Limitations
χ2-GAN [48]	Address the problem of simultaneous matching (SM) of multiple distributions.	Optimizes the divergence between μ(x, y) and μ(x)μ(y), which allows easy generalization beyond matching two distributions. Fully exploit the learned critic function.	Stable at training and embraces sample diversity during generation. Formulation generalizes to problems requiring SM of multiple distributions.	–
LSGAN [49]	Sigmoid cross entropy loss function may lead to the vanishing gradients problem. Basic GANs cause almost no loss for samples that lie in a long way on the correct side of the decision boundary.	Adopted the least squares loss function for D. Penalizes the samples lying a long way to the decision boundary.	LSGANs is more stable than original GANs during the learning process.	Do not increase the variety of mode of generated visual samples and the variety of semantics of visual samples.
SoftmaxGAN [50]	As the D utilizes a logistic loss, original GANs suffer from the vanishing gradients.	Softmax cross-entropy loss. The target is to assign all probability to real data for D and to assign probability equally to all samples for G.	The stability of GANs is improved through the usage of a Softmax cross-entropy loss in the sample space.	Do not increase the variety of mode of generated visual samples and the variety of semantics of visual samples.
OT-GAN [51]	In WGAN, it is not possible to optimize over all possible 1-Lipschitz functions, leading to imperfect critic. Sinkhorn distance has biased sample gradients.	A new distance metric Mini-batch energy distance does not require Lipschitz assumption. Mini-batch energy distance uses Sinkhorn distance along with Generalized energy distance, hence has unbiased estimator.	Mini-batch energy distance remains a valid training objective even when we stop training the critic.	It requires large amounts of computation and memory.
IGAN [7]	Overtraining of D. Mode collapse of G. Gradient descent may not converge. Vulnerable to adversarial examples. GAN outputs depend on the inputs.	Present a variety of new architectural features and training procedures for GANs. • Feature Matching. • Mini-batch Discrimination. • Historical Averaging (Fictitious play). • Label-smoothing. • Virtual Batch normalization.	Feature matching's objective performs well for classification. Minibatch discrimination works well for generating realistic images. The historical average of the parameters can be updated in an online fashion, so this learning rule scales well to long time series.	Feature matching could not generate indistinguishable samples. Minibatch discrimination is computationally complex and highly sensitive to the selection of hyperparameters. VBN has high computational complexity.
McGAN [52]	Impact of the distance choice on the stability of the optimization	Mean and covariance measure of distance for a critic function	Stable to train, have a reduced mode dropping, and the IPM loss correlates with the quality of the generated samples.	The use of clipping ends up restricting the capacity of the model. Requires matrix (tensor) decompositions, which is hard to scale to higher order moment matching.

(Continued)

Table 9. Continued

Models	Concerns Raised	Approach	Strengths	Limitations
MMD GAN [53]	GMMN is not efficient as GANs on challenging and large benchmark datasets. GMMN requires large batch size during the training.	Introduce adversarial kernel learning techniques, as the replacement of a fixed Gaussian kernel in the original GMMN.	New distance measure in MMD GAN is a meaningful loss that enjoys the advantage of weak topology and can be optimized via gradient descent with relatively small batch sizes.	Computational complexity of MMDGAN increases as number of sample increases.
CramerGAN [54]	Non-convergence of WGAN due to biased gradient estimator. Powerful critic is needed and also should not overfit the empirical distribution.	Propose Cramer distance with unbiased sample gradients. Cramer distance enables learning without perfect critic.	It measures energy distance indirectly in the data manifold but with a transformation function h.	–

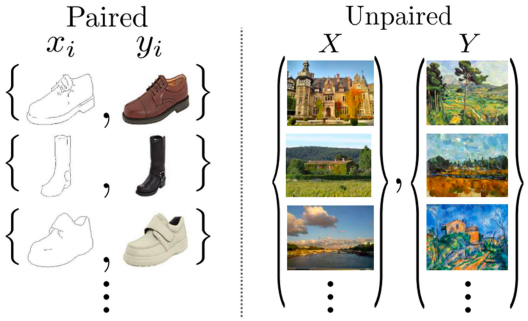

Fig. 1. Paired data vs. Unpaired data.

consider this into account, a novel **Geometry-Aware GANs model (GAGAN)** is proposed, which incorporates geometric information into the image generation process. Reference [86] proposed an adversarial image generation model, called LR-GAN, to generate sharp images by considering both scene structure and context. Unlike existing models for image generation, LR-GAN combines foregrounds on the background in a contextually relevant style for generating more realistic images. Results have shown that LR-GAN outperforms DCGAN. Reference [87] proposed **Style and Structure GAN (S2-GAN)**, model in which a GANs is used to produce the image structure and then output is fed into the second GANs for considering the image style. Generation of realistic images has a wide range of practical applications, such as anime character generation [88–93], image synthesis [94–97], super resolution [98–108], inpainting [109–112], interactive image generation [113, 114], human pose estimation [115, 116], 3D object detection [117–120], and so on.

4.2 Domain Transfer

Image-to-image translation maps an image from one domain to a corresponding image in another domain. Existing researches for image-to-image translation have used supervised setting, as shown in Figure 1 (left side), paired images (x_i, y_i) [87, 121–124]. But availability of the paired data is either difficult or expensive. Only a few datasets are available for some tasks, like semantic segmentation [125], but they are quite small. Therefore, in recent times, several researchers have proposed to translate between domains without paired dataset (see Figure 1 (right side), unpaired data

Table 10. Summary of Regularization Schemes

Models	Concerns Raised	Approach	Strengths	Limitations
WGAN-GP [55]	Weight clipping in WGAN causes vanishing and exploding gradients and capacity underuse.	WGAN except no weight clipping. Introduced a data dependent constraint. Namely. a gradient penalty to enforce the Lipschitz constraint on the critic. Added a regularization term to encourage theoretical guarantee.	Makes training more stable than WGAN and converge better. Produces high quality images.	Gradient penalty adds computational complexity.
BWGAN [56]	Extended WGAN-GP concept to any separable complete normed space.	l2 norm is replaced with a dual norm. Generalized the WGAN-GP theory to Banach spaces to allow features selection for G.	Introduced a generalization of WGANs with gradient norm penalization to Banach spaces, allowing to easily implement WGANs for a wide range of underlying norms on images.	–
CT-GAN [57]	WGAN-GP needs a lot of iterations to ensure Lipschitz constraint.	Add a regularization through Consistency term by perturbing the real data sample itself, twice.	Better photo-realistic samples than the previous methods. Achieves state-of-the-art semi-supervised learning results.	–
SN-GAN [12]	Weight clipping reduced the rank of the weight matrix. WGAN-GP introduces regularization based on unreliable model samples.	Regularization that performs spectral normalization of weight matrix and does not affect the rank.	Not dependent on model samples and less computationally complex.	–
[58]	Dimensionality misspecification. Variance due to noise.	Adding high dimensional noise. Noise-induced regularization scheme.	Regularization turns GAN models into reliable building blocks for deep learning.	–
FisherGAN [59]	Weight clipping reduces the capacity of D. WGAN-GP has high computational cost.	Introduce data-dependent regularization, which maintains the capacity of the critic while ensuring stability.	It reduces the distance between two distributions as well as in-class variance. It does not add any weight clipping or gradient penalty.	–
[60]	Revisited the basic GANs algorithm for finding the Nash-equilibrium. Non-convergence of SGD.	Identify the cause based on the Jacobian of gradients. Propose consensus optimization based on regularization w.r.t. ϕ, θ. Introduced a new design for the GANs training. Prove its convergence.	Enables stable training of GANs on a variety of architectures and divergence measures.	–

(Continued)

Table 10. Continued

Models	Concerns Raised	Approach	Strengths	Limitations
Unrolled GANs [61]	Mode collapse, as D cannot be trained till optimality at every iteration. G moves mass to a single point and D assigns lower probability to it.	Introduce a surrogate loss, which in limit equals the optimal D. G is updated based on the future update of D, hence reducing mode collapse.	Unrolling effectively increases the capacity of the D.	Computational Complexity due to k-step D's updates. Only considered a small fraction of the design space.
[62]	GAN is not convex-concave objective, hence gradient descent may not converge. WGAN has non-convergent limit cycles. Local instability in GANs.	Use ODE method to prove that GAN objective is locally asymptotically stable under certain conditions. Propose regularization on gradients of D for stability.	Regularization term guarantees local stability for both the WGAN and the traditional GANs. Speeding up convergence and addressing mode collapse.	–
[63]	Non-convergence of unregularized GANs and WGAN-GP on non-overlapping manifolds	Noise-induced regularization (Roth et al., 2017) converges. Propose simplified version of the above and prove convergence.	(Unregularized) Gradient-based GAN optimization is not always locally convergent. WGANs and WGAN-GP do not always lead to local convergence, whereas instance noise and zero-centered gradient penalties do.	–
DRAGAN [64]	Mode Collapse due to non-convex loss function. Non-convergence of alternative gradient descent. GANs learn swiss roll distribution despite vanishing gradients. WGAN-GP does not follow from KR duality as WGAN does.	View the GANs optimization as regret minimization. Prove convergence for the convex-concave case. Converge to ϵ-approximate equilibrium in non-convex case.	Avoid the local equilibria, which causes sharp D's gradients nearby some real data points.	Do not improve diverse image generation with real datasets.

(X, Y)) by exploring the underlying relationship between the domains. Image-to-image translation is categorized into two parts: unsupervised image-to-image translation and semi-supervised image-to-image translation.

Unsupervised Image-to-image translation problem is quite challenging, as unpaired data has no corresponding images. Basic GANs is designed to learn the data distribution of a domain, but image-to-image translation requires matching the joint distribution of image-image pairs. Conditional GANs can only be used to produce images of different style rather than producing images in two different domains, such as color and depth image domains. In recent times, several researchers have explored both unsupervised [126–135] and semi-supervised image-to-image translation [136–138].

Table 11. Summary of Addressed GANs Challenges and Their Proposed Solutions

Models	MC	NC&I	S_{11}	S_{12}(i)	S_{12}(ii)	S_{12}(iii)	S_{13}(i)	S_{13}(ii)	S_{14}	S_{15}	S_{16}	S_{21}	S_{22}
cGANs [1]	√		√										
LAPGAN [65]	√		√										
SGAN [66]	√		√										
BiCoGAN [3]	√		√										
MatAN [4]	√		√										
[67]	√		√										
AC-GAN [6]	√		√										
TripleGAN [68]	√		√										
KDGAN [69]	√		√										
ControlGAN [9]	√		√										
DCGANs [13]		√		√									
ProgressGAN [14]	√	√		√									
PacGAN [15]	√			√									
BayesianGAN [17]	√			√									
CapsNets [18]	√			√									
SAGAN [19]		√		√									
cGAN [70]	√				√								
AdaGAN [71]	√	√			√								
MAD-GAN [72]	√				√								
MGAN [73]	√				√								
MPM GAN [74]	√				√								
Fictitious GAN [75]	√				√								
MIX+GAN [76]	√				√								
D2GAN [21]	√					√							
GMAN [20]	√					√							
StabGAN [77]		√				√							
Dropout GAN [78]	√					√							
SGAN [22]	√	√				√							
VAE-GAN [27]	√						√						
AAE [28]	√						√						
AVB [29]	√						√						
ASVAE [31]	√						√						
MDGAN [26]	√						√						
Dist-GAN [30]	√						√						
α-GAN [32]	√						√						
ALI [33]/ **BiGAN** [34]								√					
HALI [36]								√					
AGE [37]	√							√					
VEEGAN [38]	√							√					
MGGAN [39]	√							√					
EBGAN [79]	√	√							√				
BEGAN [80]	√	√							√				
MAGAN [81]		√							√				

(Continued)

Table 11. Continued

Models	MC	NC&I	S_{11}	S_{12}(i)	S_{12}(ii)	S_{12}(iii)	S_{13}(i)	S_{13}(ii)	S_{14}	S_{15}	S_{16}	S_{21}	S_{22}
Max-Boost-GAN [82]	√	√							√				
MemoryGAN [83]		√								√			
DeliGAN [42]	√										√		
NEMGAN [40]	√										√		
DE-GAN [84]		√									√		
InfoGAN [41]		√									√		
WGAN [43]	√	√										√	
LS-GAN [44]		√										√	
RWGAN [45]		√										√	
f-GAN [46]/**b-GAN** [47]		√										√	
χ**2-GAN** [48]	√	√										√	
LSGAN [49]		√										√	
SoftmaxGAN [50]		√										√	
OT-GAN [51]		√										√	
IGAN [7]	√	√										√	
McGAN [52],		√										√	
MMD GAN [53]		√										√	
CramerGAN [54]		√										√	
WGAN-GP [55]		√											√
BWGAN [56]		√											√
CT-GAN [57]		√											√
SN-GAN [12]		√											√
[58]		√											√
FisherGAN [59]		√											√
[60]		√											√
Unrolled GANs [61]	√												√
[62]		√											√
[63]		√											√
DRAGAN [64]	√	√											√

4.3 Sequential Data Generation

It is very beneficial to have large labelled dataset for better predictive learning through neural networks. But, labelling large datasets is time-consuming and expensive. One possible solution is proposed by **Simulated + Unsupervised (S+U)** learning approach [130], in which it suggests to generate synthetic images from unlabelled real data. Moreover, S+U preserves annotation information for training of machine learning models.

In addition, the task of generating music is quite different than image and video generation, as it is only temporal data. Moreover, music is composed of various instruments with different temporal dynamics. Reference [139] proposed a GANs-based framework for symbolic multi-track music generation. Reference [140] introduced a GANs-based model to produce melodies either from scratch by following a chord sequence or by conditioning on the melody of previous bars. Moreover, authors also claimed that proposed model can be expanded to produce music with multiple MIDI channels (i.e., tracks).

However, enhancing speech is one of the possible solutions for improving speech quality in noisy environments. Recently, deep neural networks have been used to learn complex functions

from large example sets and have performed well in comparison to traditional approaches for speech enhancements. Reference [141] explored the basic feats of conditional GANs to learn mapping between spectrogram of noisy speech and its enhanced counterpart. Reference [142] proposed to operate at the waveform level and trained an end-to-end model for 28 speakers and with 40 different noise conditions.

4.4 GANs for Ethics in AI

Ethics in AI has become one of the significant areas of research. Deep learning–based software can cause threats to privacy, democracy, and national security [143]. Recent developments in generative data modeling have raised concern about several ethical issues, such as generating fake content (i.e., deepfake), privacy breaching, biased outcomes (i.e., fairness), and so on. GANs has also been explored for identifying the fake contents, handling privacy issues in the data generation, and handling bias in the data. In this sub-section, we shall point out several GANs-based solutions introduced to handle mentioned ethical issues.

4.4.1 Deepfakes. GANs generates high-quality data (text, image, video, speech) that can be used to generate fake information, i.e., deepfakes. Deepfakes algorithms generate fake images and videos whose authenticity cannot be distinguished from the real data. Deepfakes mainly have been explored for facial manipulation, which can be classified into three categories: (1) face synthesis is about creating non-existent realistic faces using GANs [144, 145]; (2) face swap is about swapping faces [146]; (3) facial attributes and expression [128] is about manipulating attributes of the face, such as color tone, age, gender, and so on. There is a need of algorithms that can detect fake content automatically. Reference [143] proposed a novel solution to detect deepfakes by identifying subtle visual artifacts in the image.

4.4.2 Handling Privacy Issues in Data Generation. GANs has also been used for generating synthetic data that can be made available publicly instead of real data. However, an adversary can get the training set membership through the GANs model and generated synthetic data. A model memorizes the training samples, which leads the issue of privacy and makes the GANs model vulnerable. Reference [147] has shown that it is easy to identify the training samples through the observation that D is more likely to classify training samples as real rather than samples not present in the training data. To achieve the privacy, records in the data can be de-identified, but now de-identified records can be re-identified by relating them to other identifiable datasets. References [148, 149] proposed **Differentially Private Generative Adversarial Network (DP-GAN)** to guarantee differential privacy of D by introducing noise during the model optimization. But, proposed model does not maintain tradeoff between sample quality and diversity while supporting differential privacy. Hence, model is not useful for practical applications. References [150–152] proposed an architecture design maintaining tradeoff between privacy and sample quality.

4.4.3 Fairness. Recently, achieving fairness in learning models has gained momentum in machine learning for several applications, such as granting loan, shortlisting candidate for interview, and so on. Decision-making models still may suffer from unwanted discrimination against sensitive attributes, such as gender, race, age, and so on. To achieve fairness in the outcome, it is important to get the unbiased training data. How to get fair training data is an important research problem.

Reference [153] proposed a GANs-based approach to generate fair dataset w.r.t. sensitive attributes in allocative decision making from the real dataset for model training. Reference [154] proposed reinforcement learning–based race balance network to handle the bias in the data. Reference [155] pointed out that existing deep learning models for face recognition encode gender

information implicitly. To handle this, an algorithm is introduced to reduce gender information from the face descriptors. Reference [156] introduced a new direction for handling the issue of missing fairness in the outcome. Authors proposed to achieve fairness through representation learning as it removes the semantics of the sensitive attributes. Reference [157] identified that existing deep learning classifiers trained to generate diagnostic labels from X-ray images are biased w.r.t. sensitive attributes. Reference [158] introduced a framework based on conditional GANs for generating synthetic fair data with selective properties from real data. Reference [159] studied fairness from the perspective of causal relations in data.

4.5 Others

Steganalysis allows to find any payload hidden in the message and retrieving it if possible. An efficient classifier is required to classify the presence of hidden payloads. Reference [160] proposed a DCGAN-based approach to produce more steganalysis-secure message embedding. Detection of small objects is a challenging task because of object's low resolution and noisy representation. Several researches have proposed to identify small objects by learning representations of all objects at multiple scales. But, these solutions are computationally expensive. To handle this issue, Reference [161] proposed a new Perceptual Generative Adversarial Network [162] model for detecting small objects by reducing the representation difference between small objects and large ones. Reference [162] proposed to use GANs for the information retrieval. Reference [165] used GANs for automatically generating accurate driving scenes for testing the reliability of DNN-based autonomous driving systems. Reference [164] used GANs for the spatio-temporal data prediction, such as taxi demand. Reference [165] proposed to produce GANs-based malware that can sidestep the black-box machine learning–based detection models.

REFERENCES

[1] M. Mirza and S. Osindero. 2014. Conditional generative adversarial nets. *arXiv preprint arXiv1411.1784*.

[2] G. Perarnau, J. van de Weijer, B. Raducanu, and J. M. Álvarez. 2016. Invertible conditional GANs for image editing. *arXiv preprint arXiv1611.06355*.

[3] A. Jaiswal, W. AbdAlmageed, Y. Wu, and P. Natarajan. 2019. Bidirectional conditional generative adversarial networks. *Lect. Notes Comput. Sci. (including Subser. Lect. Notes Artif. Intell. Lect. Notes Bioinf)*, 11363 LNCS, 216–232.

[4] G. Máttyus and R. Urtasun. 2018. Matching adversarial networks. In *Proceedings of the IEEE Computer Society Conference on Computer Vision and Pattern Recognition*. 8024–8032.

[5] H. Kwak and B.-T. Zhang. 2016. Ways of conditioning generative adversarial networks. *arXiv preprint arXiv1611.01455*.

[6] A. Odena, C. Olah, and J. Shlens. 2017. Conditional image synthesis with auxiliary classifier gans. In *Proceedings of the 34th International Conference on Machine Learning*. 4043–4055.

[7] T. Salimans, I. Goodfellow, W. Zaremba, V. Cheung, A. Radford, and X. Chen. 2016. Improved techniques for training GANs. In *Proceedings of the Conference on Advances in Neural Information Processing Systems*. 2234–2242.

[8] Z. Wang, E. P. Simoncelli, and A. C. Bovik. 2003. Multi-scale structural similarity for image quality assessment. In *Proceedings of the Asilomar Conference on Signals, Systems and Computers*. 1398–1402.

[9] M. Lee and J. Seok. 2019. Controllable generative adversarial network. *IEEE Access* 7 (2019), 28158–28169.

[10] S. Ioffe and C. Szegedy. 2015. Batch normalization: Accelerating deep network training by reducing internal covariate shift. In *Proceedings of the 32nd International Conference on Machine Learning*. 448–456.

[11] J. L. Ba, J. R. Kiros, and G. E. Hinton. 2016. Layer Normalization. *arXiv preprint arXiv:1607.06450*.

[12] T. Miyato, T. Kataoka, M. Koyama, and Y. Yoshida. 2018. Spectral normalization for generative adversarial networks. In *Proceedings of the 6th International Conference on Learning Representations*.

[13] A. Radford, L. Metz, and S. Chintala. 2016. Unsupervised representation learning with deep convolutional generative adversarial networks. In *Proceedings of the 4th International Conference on Learning Representations*.

[14] T. Karras, T. Aila, S. Laine, and J. Lehtinen. 2018. Progressive growing of GANs for improved quality, stability, and variation. In *Proceedings of the 6th International Conference on Learning Representations*.

[15] Z. Lin, G. Fanti, A. Khetan, and S. Oh. 2018. PacGan: The power of two samples in generative adversarial networks. In *Proceedings of the Conference on Advances in Neural Information Processing Systems*. 1498–1507.

[16] D. J. Im, C. D. Kim, H. Jiang, and R. Memisevic. 2016. Generating images with recurrent adversarial networks. *arXiv preprint arXiv1602.05110*.
[17] Y. Saatchi and A. G. Wilson. 2017. Bayesian GAN. In *Proceedings of the Conference on Advances in Neural Information Processing Systems*. 3623–3632.
[18] A. Jaiswal, W. AbdAlmageed, Y. Wu, and P. Natarajan. 2019. CapsuleGAN: Generative adversarial capsule network. *Lect. Notes Comput. Sci. (including Subser. Lect. Notes Artif. Intell. Lect. Notes Bioinf.)*, 11131 LNCS, 526–535.
[19] A. Zhang, Han Goodfellow, Ian Metaxas, Dimitris Odena. 2018. Self-attention generative adversarial networks. *arXiv preprint arXiv1805.08318*.
[20] I. Durugkar, I. Gemp, and S. Mahadevan. 2019. Generative multi-adversarial networks. In *Proceedings of the 5th International Conference on Learning Representations*.
[21] T. D. Nguyen, T. Le, H. Vu, and D. Phung. 2017. Dual discriminator generative adversarial nets. In *Proceedings of the Conference on Advances in Neural Information Processing Systems*. 2671–2681.
[22] T. Chavdarova and F. Fleuret. 2018. SGAN: An alternative training of generative adversarial networks. In *Proceedings of the IEEE Computer Society Conference on Computer Vision and Pattern Recognition*. 9407–9415.
[23] A. van den Oord et al. 2016. WaveNet: A generative model for raw audio. *arXiv preprint arXiv1609.03499*.
[24] A. van den Oord, N. Kalchbrenner, and K. Kavukcuoglu. 2016. Pixel recurrent neural networks. In *Proceedings of the 33rd International Conference on Machine Learning*. 2611–2620.
[25] A. van den Oord, N. Kalchbrenner, O. Vinyals, L. Espeholt, A. Graves, and K. Kavukcuoglu. 2016. Conditional image generation with PixelCNN decoders. In *Proceedings of the Conference on Advances in Neural Information Processing Systems*. 4797–4805.
[26] T. Che, Y. Li, A. P. Jacob, Y. Bengio, and W. Li. 2019. Mode regularized generative adversarial networks. In *Proceedings of the 5th International Conference on Learning Representations*.
[27] A. B. L. Larsen, S. K. Sønderby, H. Larochelle, and O. Winther. 2016. Autoencoding beyond pixels using a learned similarity metric. *33rd International Conference on Machine Learning*. 2341–2349.
[28] A. Makhzani, J. Shlens, N. Jaitly, I. Goodfellow, and B. Frey. 2017. Adversarial autoencoders. *arXiv preprint arXiv1511.05644*.
[29] L. Mescheder, S. Nowozin, and A. Geiger. 2017. Adversarial variational Bayes: Unifying variational autoencoders and generative adversarial networks. In *Proceedings of the 34th International Conference on Machine Learning*. 3694–3707.
[30] N. T. Tran, T. A. Bui, and N. M. Cheung. 2018. Dist-GAN: An improved GAN using distance constraints. *Lect. Notes Comput. Sci. (including Subser. Lect. Notes Artif. Intell. Lect. Notes Bioinf.)*, 11218 LNCS, 387–401.
[31] Y. Pu et al. 2017. Adversarial symmetric variational autoencoder. *arXiv preprint arXiv:1711.04915*.
[32] M. Rosca, B. Lakshminarayanan, D. Warde-Farley, and S. Mohamed. 2017. Variational approaches for auto-encoding generative adversarial networks. *arXiv preprint arXiv1706.04987*.
[33] V. Dumoulin et al. 2019. Adversarially learned inference. In *Proceedings of the 5th International Conference on Learning Representations*.
[34] J. Donahue, T. Darrell, and P. Krähenbühl. 2016. Adversarial feature learning. *arXiv preprint arXiv:1605.09782*.
[35] I. J. Goodfellow et al. 2014. Generative adversarial nets. In *Proceedings of the Conference on Advances in Neural Information Processing Systems*. 2672–2680.
[36] M. I. Belghazi, S. Rajeswar, O. Mastropietro, N. Rostamzadeh, J. Mitrovic, and A. Courville. 2018. Hierarchical adversarially learned inference. *ArXiv preprint arXiv1802.01071*.
[37] D. Ulyanov, A. Vedaldi, and V. Lempitsky. 2018. It takes (only) two: Adversarial generator-encoder networks. In *Proceedings of the 32nd AAAI Conference on Artificial Intelligence*. 1250–1257.
[38] A. Srivastava, L. Valkov, C. Russell, M. U. Gutmann, and C. Sutton. 2017. VEEGAN: Reducing mode collapse in GANs using implicit variational learning. *arXiv preprint arXiv:1705.07761*.
[39] D. Bang and H. Shim. 2018. MGGAN: Solving mode collapse using manifold guided training. *arXiv preprint arXiv1804.04391*.
[40] D. Mishra, P. A. P. A. Jayendran, V. Srivastava, and S. Chaudhury. 2018. NEMGAN: Noise engineered mode-matching GAN. *arXiv preprint arXiv1811.03692*.
[41] X. Chen, Y. Duan, R. Houthooft, J. Schulman, I. Sutskever, and P. Abbeel. 2016. InfoGAN: Interpretable representation learning by information maximizing generative adversarial nets. In *Proceedings of the Conference on Advances in Neural Information Processing Systems*. 2172–2180.
[42] S. Gurumurthy, R. K. Sarvadevabhatla, and R. V. Babu. 2017. DeLiGAN : Generative adversarial networks for diverse and limited data. In *Proceedings of the 30th IEEE Conference on Computer Vision and Pattern Recognition*. 4941–4949.
[43] M. Arjovsky, S. Chintala, and L. Bottou. 2017. Wasserstein generative adversarial networks. In *Proceedings of the International Conference on Machine Learning*. 214–223.
[44] G.-J. Qi. 2017. Loss-sensitive generative adversarial networks on lipschitz densities. *Int. J. Comput. Vis.* 128, 5 (2017), 1118–1140.

[45] X. Guo, J. Hong, T. Lin, and N. Yang. 2017. Relaxed Wasserstein with applications to GANs. *arXiv preprint arXiv1705.07164*.
[46] S. Nowozin, B. Cseke, and R. Tomioka. 2016. f-GAN: Training generative neural samplers using variational divergence minimization. In *Proceedings of the Conference on Advances in Neural Information Processing Systems*. 271–279.
[47] M. Uehara, I. Sato, M. Suzuki, K. Nakayama, and Y. Matsuo. 2016. Generative adversarial nets from a density ratio estimation perspective. *arXiv preprint arXiv1610.02920*.
[48] C. Tao, L. Chen, R. Henao, J. Feng, and L. Carin. 2018. X2 generative adversarial network. In *Proceedings of the 35th International Conference on Machine Learning*. 7787–7796.
[49] X. Mao, Q. Li, H. Xie, R. Y. K. Lau, Z. Wang, and S. P. Smolley. 2017. Least squares generative adversarial networks. In *Proceedings of the IEEE International Conference on Computer Vision*. 2813–2821.
[50] M. Lin. 2017. Softmax GAN. *arXiv preprint arXiv1704.06191*.
[51] T. Salimans, D. Metaxas, H. Zhang, and A. Radford. 2018. Improving GANs using optimal transport. In *Proceedings of the 6th International Conference on Learning Representations*.
[52] Y. Mroueh, T. Sercu, and V. Goel. 2017. McGAN: Mean and covariance feature matching GAN. In *Proceedings of the 34th International Conference on Machine Learning*. 3885–3899.
[53] C. L. Li, W. C. Chang, Y. Cheng, Y. Yang, and B. Póczos. 2017. MMD GAN: Towards deeper understanding of moment matching network. In *Proceedings of the Conference on Advances in Neural Information Processing Systems*. 2204–2214.
[54] M. G. Bellemare et al. 2017. The Cramer distance as a solution to biased Wasserstein gradients. *arXiv preprint arXiv1705.10743*.
[55] I. Gulrajani, F. Ahmed, M. Arjovsky, V. Dumoulin, and A. Courville. 2017. Improved training of Wasserstein GANs. In *Proceedings of the Conference on Advances in Neural Information Processing Systems*. 5768–5778.
[56] J. Adler and S. Lunz. 2018. Banach Wasserstein GAN. In *Proceedings of the Conference on Advances in Neural Information Processing Systems*. 6754–6763.
[57] X. Wei, B. Gong, Z. Liu, W. Lu, and L. Wang. 2018. Improving the improved training of wasserstein GANs: A consistency term and its dual effect. *arXiv preprint arXiv1803.01541*.
[58] K. Roth, A. Lucchi, S. Nowozin, and T. Hofmann. 2017. Stabilizing training of generative adversarial networks through regularization. In *Proceedings of the Conference on Advances in Neural Information Processing Systems*. 2019–2029.
[59] Y. Mroueh and T. Sercu. 2017. Fisher GAN. In *Proceedings of the Conference on Advances in Neural Information Processing Systems*. 2514–2524.
[60] L. Mescheder, S. Nowozin, and A. Geiger. 2017. The numerics of GANs. In *Proceedings of the Conference on Advances in Neural Information Processing Systems*. 1826–1836.
[61] L. Metz, B. Poole, D. Pfau, and J. Sohl-Dickstein. 2016. Unrolled generative adversarial networks. *arXiv Preprint arXiv:1611.02163*.
[62] V. Nagarajan and J. Z. Kolter. 2017. Gradient descent GAN optimization is locally stable. In *Proceedings of the Conference on Advances in Neural Information Processing Systems*. 5586–5596.
[63] L. Mescheder, A. Geiger, and S. Nowozin. 2018. Which training methods for GANs do actually converge? In *Proceedings of the 35th International Conference on Machine Learning*. 5589–5626.
[64] N. Kodali, J. Abernethy, J. Hays, and Z. Kira. 2017. On convergence and stability of GANs. *arXiv preprint arXiv1705.07215*.
[65] E. Denton, S. Chintala, A. Szlam, and R. Fergus. 2015. Deep generative image models using a Laplacian pyramid of adversarial networks. In *Proceedings of the Conference on Advances in Neural Information Processing Systems*. 1486–1494.
[66] S. Huang, Xun Li, Yixuan Poursaeed, Omid Hopcroft, and John Belongie. 2017. Stacked generative adversarial networks. *Proceedings of the Conference on Computer Vision and Pattern Recognition*. 5077–5086.
[67] S. Liu, T. Wang, D. Bau, J.-Y. Zhu, and A. Torralba. 2020. Diverse image generation via self-conditioned GANs. In *Proceedings of the IEEE/CVF Conference on Computer Vision and Pattern Recognition*. 14274–14283.
[68] L. Chongxuan, T. Xu, J. Zhu, and B. Zhang. 2018. Triple generative adversarial nets. In *Proceedings of the Conference on Advances in Neural Information Processing Systems*. 4088–4098.
[69] X. Wang, Y. Sun, R. Zhang, and J. Qi. 2018. KDGAN: Knowledge distillation with generative adversarial networks. In *Proceedings of the Conference on Advances in Neural Information Processing Systems*. 775–786.
[70] Y. Wang, L. Zhang, and J. van de Weijer. 2017. Ensembles of generative adversarial networks. *arXiv preprint arXiv1612.00991*.
[71] I. Tolstikhin, S. Gelly, O. Bousquet, C. J. Simon-Gabriel, and B. Schölkopf. 2017. AdaGAN: Boosting generative models. In *Proceedings of the Conference on Advances in Neural Information Processing Systems*. 5425–5434.
[72] A. Ghosh, V. Kulharia, V. Namboodiri, P. H. S. Torr, and P. K. Dokania. 2018. Multi-agent diverse generative adversarial networks. In *Proceedings of the IEEE Computer Society Conference on Computer Vision and Pattern Recognition*. 8513–8521.

[73] Q. Hoang, T. D. Nguyen, T. Le, and D. Phung. 2017. Multi-generator generative adversarial nets. *arXiv preprint arXiv1708.02556*.
[74] A. Ghosh, V. Kulharia, and V. Namboodiri. 2016. Message passing multi-agent GANs. *arXiv preprint arXiv1612.01294*.
[75] H. Ge, Y. Xia, X. Chen, R. Berry, and Y. Wu. 2018. Fictitious GAN: Training GANs with historical models. In *Proceedings of the European Conference on Computer Vision (ECCV'18)*. 119–134.
[76] S. Arora, R. Ge, Y. Liang, T. Ma, and Y. Zhang. 2017. Generalization and equilibrium in generative adversarial nets (GANs). In *Proceedings of the 34th International Conference on Machine Learning*. 322–349.
[77] B. Neyshabur, S. Bhojanapalli, and A. Chakrabarti. 2017. Stabilizing GAN training with multiple random projections. *arXiv preprint arXiv1705.07831*.
[78] G. Mordido, H. Yang, and C. Meinel. 2018. Dropout-GAN: Learning from a dynamic ensemble of discriminator. *arXiv preprint arXiv:1807.11346*, 2018.
[79] J. Zhao, M. Mathieu, and Y. LeCun. 2016. Energy-based generative adversarial networks. *arXiv preprint arXiv:1609.03126*.
[80] D. Berthelot, T. Schumm, and L. Metz. 2017. BEGAN: Boundary equilibrium generative adversarial networks. *arXiv preprint arXiv1703.10717*.
[81] R. Wang, A. Cully, H. J. Chang, and Y. Demiris. 2017. MAGAN: Margin adaptation for generative adversarial networks. *arXiv preprint arXiv1704.03817*.
[82] X. Di and P. Yu. 2017. Max-boost-GAN: Max operation to boost generative ability of generative adversarial networks. In *Proceedings of the IEEE International Conference on Computer Vision Workshops*. 1156–1164.
[83] Y. Kim, M. Kim, and G. Kim. 2018. Memorization precedes generation: Learning unsupervised GANs with memory networks. *arXiv preprint arXiv:1803.01500*.
[84] G. Zhong, W. Gao, Y. Liu, and Y. Yang. 2018. Generative adversarial networks with decoder-encoder output noise. *arXiv preprint arXiv1807.03923*.
[85] J. Kossaifi, L. Tran, Y. Panagakis, and M. Pantic. 2018. GAGAN: Geometry-aware generative adversarial networks. In *Proceedings of the IEEE Conference on Computer Vision and Pattern Recognition (CVPR'18)*. 878–887.
[86] J. Yang, A. Kannan, D. Batra, and D. Parikh. 2017. LR-GAN: Layered recursive generative adversarial networks for image generation. *arXiv preprint arXiv:1703.01560*.
[87] X. Wang and A. Gupta. 2016. Generative image modeling using style and structure adversarial networks. *Lect. Notes Comput. Sci. (including Subser. Lect. Notes Artif. Intell. Lect. Notes Bioinf.)*, 9908 LNCS, 318–335.
[88] Mattya. 2015. chainer-dcgan. https://github.com/mattya/chainer-DCGAN.
[89] Hiroshiba. 2016. Girl friend factory. http://qiita.com/Hiroshiba/items/d5749d8896613e6f0b48.
[90] Jie Lei. 2017. Animegan. https://github.com/jayleicn/animeGAN.
[91] Rezoolab. 2015. Make illustration on computer with chainer. http://qiita.com/rezoolab/items/5cc96b6d31153e0c86bc.
[92] Y. Jin, J. Zhang, M. Li, Y. Tian, H. Zhu, and Z. Fang. 2017. Towards the automatic anime characters creation with generative adversarial networks. *arXiv preprint arXiv1708.05509*.
[93] R. Wu, X. Gu, X. Tao, X. Shen, Y.-W. Tai, and J. Iaya Jia. 2019. Landmark assisted cycleGAN for cartoon face generation. *arXiv preprint arXiv1907.01424*.
[94] S. Reed, Z. Akata, S. Mohan, S. Tenka, B. Schiele, and H. Lee. 2016. Learning what and where to draw. In *Proceedings of the Conference on Advances in Neural Information Processing Systems*. 217–225.
[95] S. Reed, Z. Akata, X. Yan, L. Logeswaran, B. Schiele, and H. Lee. 2016. Generative adversarial text to image synthesis. In *International Conference on Machine Learning*. 1060–1069.
[96] H. Zhang et al. 2019. StackGAN++: Realistic image synthesis with stacked generative adversarial networks. *IEEE Trans. Pattern Anal. Mach. Intell* 41, 8 (2019), 1947–1962.
[97] A. Dash, J. C. B. Gamboa, S. Ahmed, M. Liwicki, and M. Z. Afzal. 2017. TAC-GAN—Text conditioned auxiliary classifier generative adversarial network. *arXiv preprint arXiv1703.06412*.
[98] K. Nasrollahi and T. B. Moeslund. 2014. Super-resolution: A comprehensive survey. *Mach. Vis. Appl* 25, 6 (2014), 1423–1468.
[99] Y. Zhang et al. 2012. Reconstruction of super-resolution lung 4D-CT using patch-based sparse representation. In *Proceedings of the IEEE Computer Society Conference on Computer Vision and Pattern Recognition*. 925–931.
[100] A. Nguyen, J. Clune, Y. Bengio, A. Dosovitskiy, and J. Yosinski. 2017. Plug and play generative networks: Conditional iterative generation of images in latent space. In *Proceedings of the 30th IEEE Conference on Computer Vision and Pattern Recognition*. 3510–3520.
[101] W. W. W. Zou and P. C. Yuen. 2012. Very low resolution face recognition problem. *IEEE Trans. Image Proc.* 21, 1 (2012), 327–340.
[102] K. Choi, C. Kim, M.-H. Kang, and J. B. Ra. 2011. Resolution improvement of infrared images using visible image information. *IEEE Sig. Proc. Lett.* 18, 10 (2011), 611–614.

[103] C. Ledig et al. 2017. Photo-realistic single image super-resolution using a generative adversarial network. In *Proceedings of the 30th IEEE Conference on Computer Vision and Pattern Recognition*. 105–114.

[104] M. S. M. Sajjadi, B. Scholkopf, and M. Hirsch. 2017. EnhanceNet: Single image super-resolution through automated texture synthesis. In *Proceedings of the IEEE International Conference on Computer Vision*. 4501–4510.

[105] R. Mechrez, I. Talmi, F. Shama, and L. Zelnik-Manor. 2019. Maintaining natural image statistics with the contextual loss. *Lect. Notes Comput. Sci. (including Subser. Lect. Notes Artif. Intell. Lect. Notes Bioinf.)*, 11363 LNCS, 427–443.

[106] X. Deng. 2018. Enhancing image quality via style transfer for single image super-resolution. *IEEE Sig. Proc. Lett.* 25, 4 (2018), 571–575.

[107] S. Vasu, N. Thekke Madam, and A. N. Rajagopalan. 2019. Analyzing perception-distortion tradeoff using enhanced perceptual super-resolution network. *Lect. Notes Comput. Sci. (including Subser. Lect. Notes Artif. Intell. Lect. Notes Bioinf.)*, 11133 LNCS 114–131.

[108] H. Bin, C. Weihai, W. Xingming, and L. Chun-Liang. 2017. High-quality face image SR using conditional generative adversarial networks. *arXiv preprint arXiv1707.00737*.

[109] D. Pathak, P. Krahenbuhl, J. Donahue, T. Darrell, and A. A. Efros. 2016. Context encoders: Feature learning by inpainting. In *Proceedings of the IEEE Computer Society Conference on Computer Vision and Pattern Recognition*. 2536–2544.

[110] R. A. Yeh, C. Chen, T. Yian Lim, A. G. Schwing, M. Hasegawa-Johnson, and M. N. Do. 2017. Semantic image inpainting with deep generative models. In *Proceedings of the 30th IEEE Conference on Computer Vision and Pattern Recognition*. 6882–6890.

[111] E. Denton, S. Gross, and R. Fergus. 2016. Semi-supervised learning with context-conditional generative adversarial networks. *arXiv preprint arXiv1611.06430*.

[112] Y. Li, S. Liu, J. Yang, and M. H. Yang. 2017. Generative face completion. In *Proceedings of the 30th IEEE Conference on Computer Vision and Pattern Recognition*. 5892–5900.

[113] J. Y. Zhu, P. Krähenbühl, E. Shechtman, and A. A. Efros. 2016. Generative visual manipulation on the natural image manifold. *Lect. Notes Comput. Sci. (including Subser. Lect. Notes Artif. Intell. Lect. Notes Bioinf.)*, 9909 LNCS, 597–613.

[114] A. Brock, T. Lim, J. M. Ritchie, and N. Weston. 2019. Neural photo editing with introspective adversarial networks. In *Proceedings of the 5th International Conference on Learning Representations*.

[115] B. Zhao, X. Wu, Z.-Q. Cheng, H. Liu, Z. Jie, and J. Feng. 2018. Multi-view image generation from a single-view. In *Proceedings of the 26th ACM international conference on Multimedia*. 383–391.

[116] L. Ma, X. Jia, Q. Sun, B. Schiele, T. Tuytelaars, and L. Van Gool. 2017. Pose guided person image generation. In *Proceedings of the Conference on Advances in Neural Information Processing Systems*. 406–416.

[117] J. Wu, C. Zhang, T. Xue, W. T. Freeman, and J. B. Tenenbaum. 2016. Learning a probabilistic latent space of object shapes via 3D generative-adversarial modeling. In *Proceedings of the Conference on Advances in Neural Information Processing Systems*. 82–90.

[118] D. J. Rezende, S. M. Ali Eslami, S. Mohamed, P. Battaglia, M. Jaderberg, and N. Heess. 2016. Unsupervised learning of 3D structure from images. In *Proceedings of the Conference on Advances in Neural Information Processing Systems*. 5003–5011.

[119] X. Yan, J. Yang, E. Yumer, Y. Guo, and H. Lee. 2016. Perspective transformer nets: Learning single-view 3D object reconstruction without 3D supervision. In *Proceedings of the Conference on Advances in Neural Information Processing Systems*. 1704–1712.

[120] M. Gadelha, S. Maji, and R. Wang. 2018. 3D shape induction from 2D views of multiple objects. In *Proceedings of the International Conference on 3D Vision*. 402–411.

[121] E. Shelhamer, J. Long, and T. Darrell. 2017. Fully convolutional networks for semantic segmentation. *IEEE Trans. Pattern Anal. Mach. Intell.* 39, 4 (2017), 640–651.

[122] Y. Shih, S. Paris, F. Durand, and W. T. Freeman. 2013. Data-driven hallucination of different times of day from a single outdoor photo. *ACM Trans. Graph.* 32, 6 (2013), 1–11.

[123] S. Xie and Z. Tu. 2017. Holistically-nested edge detection. *Int. J. Comput. Vis.* 125, 1–3 (2017), 3–18.

[124] R. Zhang, P. Isola, and A. A. Efros. 2016. Colorful image colorization. *Lect. Notes Comput. Sci. (including Subser. Lect. Notes Artif. Intell. Lect. Notes Bioinf.)*, 9907 LNCS, 649–666.

[125] M. Cordts et al. 2016. The cityscapes dataset for semantic urban scene understanding. In *Proceedings of the IEEE Conference on Computer Vision and Pattern Recognition*. 3213–3223.

[126] M. Y. Liu and O. Tuzel. 2016. Coupled generative adversarial networks. In *Proceedings of the Conference on Advances in Neural Information Processing Systems*. 469–477.

[127] M.-Y. Liu, T. Breuel, and J. Kautz. 2017. Unsupervised Image-to-Image Translation Networks. *arXiv preprint arXiv:1703.00848*.

[128] Y. Choi, M. Choi, M. Kim, J.-W. Ha, S. Kim, and J. Choo. 2018. StarGAN: Unified generative adversarial networks for multi-domain image-to-image translation. In *Proceedings of the IEEE Conference on Computer Vision and Pattern Recognition*. 8789–8797.

[129] Y. Taigman, A. Polyak, and L. Wolf. 2019. Unsupervised cross-domain image generation. In *Proceedings of the 5th International Conference on Learning Representations*.

[130] A. Shrivastava, T. Pfister, O. Tuzel, J. Susskind, W. Wang, and R. Webb. 2017. Learning from simulated and unsupervised images through adversarial training. In *Proceedings of the IEEE conference on computer vision and pattern recognition*. 2107-2116.

[131] K. Bousmalis et al. 2017. Unsupervised Pixel-Level Domain Adaptation with Generative Adversarial Networks. In *Proceedings of the IEEE Conference on Computer Vision and Pattern Recognition*. 3722–3731.

[132] J.-Y. Zhu, T. Park, P. Isola, A. A. Efros, and B. A. Research. Unpaired image-to-image translation using cycle-consistent adversarial networks monet photos. In *Proceedings of the IEEE International Conference on Computer Vision*. 2223–2232.

[133] Z. Yi, H. Zhang, P. Tan, and M. Gong. DualGAN: Unsupervised dual learning for image-to-image translation. In *Proceedings of the IEEE International Conference on Computer Vision*. 2849–2857.

[134] Y. Pu et al. 2018. JointGAN: Multi-domain joint distribution learning with generative adversarial nets. In *International Conference on Machine Learning*. 4151–4160.

[135] C. Du, C. Du, X. Xie, C. Zhang, and H. Wang. 2018. Multi-view adversarially learned inference for cross-domain joint distribution matching. In *Proceedings of the 24th ACM SIGKDD International Conference on Knowledge Discovery and Data Mining*. 1348–1357.

[136] Z. Gan et al. 2017. Triangle Generative Adversarial Networks. *arXiv preprint arXiv:1709.06548*.

[137] Z. Deng et al. 2017. Structured Generative Adversarial Networks. *arXiv preprint arXiv:1711.00889*.

[138] J. Yoon, J. Jordon, and M. Schaar. 2018. RadialGAN: Leveraging multiple datasets to improve target-specific predictive models using generative adversarial networks. In *International Conference on Machine Learning*. 5699–5707.

[139] H. W. Dong, W. Y. Hsiao, L. C. Yang, and Y. H. Yang. 2018. MuseGAN: Multi-track sequential generative adversarial networks for symbolic music generation and accompaniment. In *Proceedings of the 32nd AAAI Conference on Artificial Intelligence*. 34–41.

[140] L. C. Yang, S. Y. Chou, and Y. H. Yang. 2017. MidiNet: A convolutional generative adversarial network for symbolic-domain music generation. In *Proceedings of the 18th International Society for Music Information Retrieval Conference*. 324–331.

[141] D. Michelsanti and Z. H. Tan. 2017. Conditional generative adversarial networks for speech enhancement and noise-robust speaker verification. In *Proceedings of the Conference of the International Speech Communication Association*. 2008–2012.

[142] S. Pascual, A. Bonafonte, and J. Serra. 2017. SEGAN: Speech enhancement generative adversarial network. In *Proceedings of the Conference of the International Speech Communication Association*. 3642–3646.

[143] L. Chai, D. Bau, S.-N. Lim, and P. Isola. 2020. What makes fake images detectable? Understanding properties that generalize. *arXiv preprint arXiv2008.10588*.

[144] T. Karras, S. Laine, and T. Aila. 2019. A style-based generator architecture for generative adversarial networks. In *Proceedings of the IEEE Computer Society Conference on Computer Vision and Pattern Recognition*. 4396–4405.

[145] H. Dang, F. Liu, J. Stehouwer, X. Liu, and A. Jain. 2019. On the detection of digital face manipulation. In *Proceedings of the IEEE/CVF Conference on Computer Vision and Pattern Recognition*. 5781–5790.

[146] A. Rössler, D. Cozzolino, L. Verdoliva, C. Riess, J. Thies, and M. Nießner. 2019. FaceForensics++: Learning to detect manipulated facial images. *Proceedings of the International Conference on Computer Vision*. 1–11.

[147] J. Hayes, L. Melis, G. Danezis, and E. De Cristofaro. 2017. LOGAN: Membership inference attacks against generative models. *Proc. Priv. Enhanc. Technol.* 1 (2019), 133–152.

[148] A. Narayanan and V. Shmatikov. 2008. Robust de-anonymization of large sparse datasets. In *Proceedings of the IEEE Symposium on Security and Privacy*. 111–125.

[149] L. Xie, K. Lin, S. Wang, F. Wang, and J. Zhou. 2018. Differentially private generative adversarial network. *arXiv preprint arXiv1802.06739*.

[150] S. Mukherjee, Y. Xu, A. Trivedi, and J. L. Ferres. PrivGAN: Protecting GANs from membership inference attacks at low cost. *arXiv preprint arXiv:2001.00071*.

[151] J. Jordon, J. Yoon, and M. Van Der Schaar. PATE-GAN: Generating synthetic data with differential privacy guarantees. In *Proceedings of the International Conference on Learning Representations*.

[152] Y. Liu, J. Peng, J. J. Q. Yu, and Y. Wu. 2019. PPGAN: Privacy-preserving generative adversarial network. In *Proceedings of the IEEE 25th International Conference on Parallel and Distributed Systems*.

[153] P. Sattigeri, S. C. Hoffman, V. Chenthamarakshan, and K. R. Varshney. 2019. Fairness GAN. *arXiv preprint arXiv1805.09910*.

[154] M. Wang and W. Deng. 2019. Mitigate bias in face recognition using skewness-aware reinforcement learning. *arXiv preprint arXiv:1911.10692*.

[155] P. Dhar, J. Gleason, H. Souri, C. D. Castillo, and R. Chellappa. 2020. An adversarial learning algorithm for mitigating gender bias in face recognition. *arXiv preprint arXiv:2006.07845*.

[156] N. Quadrianto, V. Sharmanska, and O. Thomas. 2018. Discovering fair representations in the data domain. In *Proceedings of the IEEE Computer Society Conference on Computer Vision and Pattern Recognition*. 8219–8228.

[157] L. Seyyed-Kalantari, G. Liu, M. McDermott, and M. Ghassemi. 2020. CheXclusion: Fairness gaps in deep chest X-ray classifiers. In *Proceedings of the Pacific Symposium of BIOCOMPUTING*. 232–243.

[158] A. Abusitta, E. Aïmeur, and O. A. Wahab. 2019. Generative adversarial networks for mitigating biases in machine learning systems. *arXiv preprint arXiv1905.09972*.

[159] D. Xu, Y. Wu, S. Yuan, L. Zhang, and X. Wu. 2019. Achieving causal fairness through generative adversarial networks. In *Proceedings of the 28th International Joint Conference on Artificial Intelligence*. 1452–1458.

[160] D. Volkhonskiy, I. Nazarov, and E. Burnaev. 2020. Steganographic generative adversarial networks. In *Proceedings of the 12thInternational Conference on Machine Vision*.

[161] J. Li, X. Liang, Y. Wei, T. Xu, J. Feng, and S. Yan. 2017. Perceptual generative adversarial networks for small object detection. In *Proceedings of the 30th IEEE Conference on Computer Vision and Pattern Recognition*. 1951–1959.

[162] W. Zhang. 2018. Generative adversarial nets for information retrieval: Fundamentals and advances. In *Proceedings of the 41st International ACM SIGIR Conference on Research and Development in Information Retrieval*. 1375–1378.

[163] M. Zhang, Y. Zhang, L. Zhang, C. Liu, and S. Khurshid. 2018. DeepRoad: GAN-based metamorphic autonomous driving system testing. In *Proceedings of the 33rd ACM/IEEE International Conference on Automated Software Engineering*. 132–142.

[164] D. Saxena and J. Cao. 2019. D-GAN: Deep generative adversarial nets for spatio-temporal prediction. *arXiv preprint arXiv1907.08556*.

[165] W. Hu and Y. Tan. 2017. Generating adversarial malware examples for black-box attacks based on GAN. *arXiv preprint arXiv1702.05983*.